Desalination and Water Treatment
www.deswater.com

doi: 10.5004/dwt.2020.25260

183 (2020) 104–113
April

Performance analysis of serially-connected membrane element for pressure-assisted forward osmosis: wastewater reuse and seawater desalination

Chulmin Lee[a], Nguyen Thanh Tin[a], Rusnang Syamsul Adha[a], In S. Kim[b,*]

[a]*School of Earth Sciences and Environmental Engineering, Gwangju Institute of Science and Technology (GIST), 123 Cheomdangwagi-ro, Buk-gu, Gwangju 61005, Korea*
[b]*Global Desalination Research Centre, Gwangju Institute of Science and Technology (GIST), 123 Cheomdangwagi-ro, Buk-gu, Gwangju 61005, Korea, Tel. +82-62-715-2436; email: iskim@gist.ac.kr*

Received 23 August 2019; Accepted 25 November 2019

ABSTRACT

Forward osmosis-reverse osmosis (FO-RO) hybrid process has gained much research attention as a promising alternative to reduce energy consumption and overall plant cost of conventional stand-alone seawater reverse osmosis. Furthermore, pressure-assisted forward osmosis-reverse osmosis (PAFO-RO) hybrid has been suggested to further improve FO water flux and enhance draw stream dilution. Several pilot-based performance analyses and economic assessments using commercial FO modules have been reported to validate the feasibility of this hybrid process in recent years. However, FO/PAFO performance evaluated using real seawater and wastewater has been hardly reported, especially regarding the effect of hydraulic operating conditions. The current study was dedicated to provide a performance analysis of serially-connected FO 8040 spiral-wound element under a broad range of feed, draw flowrate and hydraulic pressure. The results revealed that there was no significant improvement in water flux above 20 LPM of feed flowrate and 5 LPM of draw flowrate regardless of hydraulic pressure and number of elements in a serial configuration. In addition, a significant discrepancy of PAFO performance between artificial and field water conditions was observed. Overall water flux under field water condition was almost half of that under artificial water condition. Diluted concentration showed a relatively smaller discrepancy between the conditions, yet, this performance difference can potentially alter the economic feasibility of the FO-RO or PAFO-RO hybrid process. The result and discussion in this study imply that economic assessment based on artificial water conditions can misrepresent the actual economic feasibility of the hybrid process.

Keywords: Pressure assisted forward osmosis; Forward osmosis; Spiral-wound element; Economic feasibility; Desalination

1. Introduction

Forward osmosis (FO) is the osmotically-driven process that utilizes the salinity gradient between two solutions to permeate water through a selective semi-permeable membrane [1]. Since its first invention, FO has been reintroduced to the desalination field as a potential alternative to seawater reverse osmosis (SWRO) and actively been studied in the last decade. However, it turned out the stand-alone FO process was not able to overcome its inherent limitation, high energy requirement in draw solutes recovery for retrieving pure water from diluted draw solution, undermining feasibility of FO compared to conventional SWRO in economic aspect [2]. Nevertheless, FO has been suggested again as a pretreatment of SWRO to dilute seawater by utilizing impaired water sources as feed to reduce intensive energy

* Corresponding author.

Presented at the 12th International Desalination Workshop (IDW2019), 28–30 August 2019, Jeju, Korea

This article was originally published with an error in the grant number in Acknowledgment section. This version has been corrected. Please see Corrigendum in vol. 186 (2020) 464 [10.5004/dwt.2020.26074].

demand in following RO operation, so-called FO-RO hybrid process [3].

Meanwhile, to further improve the economics of FO-RO hybrid, pressure-assisted forward osmosis (PAFO) has been studied in recent years to enhance dilution of draw stream by applying moderate hydraulic pressure, allowing to achieve higher water flux [4–6]. PAFO-RO hybrid is expected to further reduce energy cost in the following RO process by enhanced dilution of RO feed concentration compared to the FO-RO scheme. The additional energy consumption for pressurizing the feed stream can have a negative impact on the FO operating expenditure (OPEX), however, this loss of OPEX can be compensated by a reduction of FO capital expenditure, especially reduced FO membrane area.

To examine the economic feasibility of FO-RO hybrid, recent pilot-based studies [7–10] reported the performance of commercial FO spiral-wound and plate and frame modules using artificial seawater as draw and tap water as feed under varying operating conditions. Furthermore, some economic assessments were attempted to evaluate the feasibility of FO-RO hybrid compare to conventional processes, however, with a limitation that assessments were based on the performance of lab-scale tests using membrane coupons, a large portion of components in economic assessment remain uncertain [11,12]. On this wise, one study [13] conducted an economic assessment of PAFO-RO hybrid process based on pilot-scale PAFO operation using artificial seawater as draw and tap water as feed. However, the performance of FO evaluated using artificial solutions can misrepresent practical FO performance since on-site performance evaluated using real seawater and wastewater can create discrepancy due to different characteristics of feed and draw solutions. Therefore, pilot-scale performance evaluation of the PAFO process under realistic feed and draw conditions needs to be evaluated for more practical and reliable feasibility of the PAFO-RO hybrid process. Up to date, there is only one study reporting pilot-scale FO performance under non-artificial feed and draw conditions [14], nonetheless, performance analysis of FO and PAFO operation using non-artificial solutions is still severely limited.

The objective of this study is to conduct performance analysis using a single and multiple spiral-wound FO elements in a serial configuration under in an extensive range of feed, draw flowrates and hydraulic pressure. The resulting water flux patterns and degrees of dilution of draw solution were systematically analysed in association with effect of each operating condition. Furthermore, performance discrepancy from different water chemistry between artificial solutions and realistic seawater and wastewater was discussed.

2. Material and methods

2.1. FO spiral wound element

The spiral-wound FO element (CSM FO-8040, Toray Chemical Korea Inc., Korea) was used for the pilot-scale operation. The FO element consists of 12 layers of membrane leaves that include two polyamide thin-film composite (PA-TFC) flat sheet membranes, two layers of tricot fine spacers and a diamond-shaped spacer in the center enveloped by the two fine spacers. The total effective membrane area of one element was 15.3 m^2. A detailed description of the characteristics of the membrane can be found elsewhere. Also, illustration of the structural characteristics of the element is shown in Fig. 1.

2.2. Characteristic of secondary wastewater effluent and seawater

Secondary effluent from the wastewater treatment plant and raw seawater were pre-treated with mesh tube filtration and cartridge filter to be utilized as feed and draw solution in following PAFO operation. Each water quality parameter of feed and draw solutions was measured before and after pretreatment is listed in Table 1. Total organic carbon (TOC) was measured using a TOC analyzer (TOC-L, Shimadzu, Japan). Due to high organic fouling contents, the silt density index (SDI) was not able to be measured in secondary effluent. Suspended solids (SS) and SDI were determined by the following procedure of standard methods (ASTM, 2014).

2.3. FO pilot system design

Fig. 1 illustrates schematic diagram of the PAFO pilot system set-up. There are four liquid transfer pumps

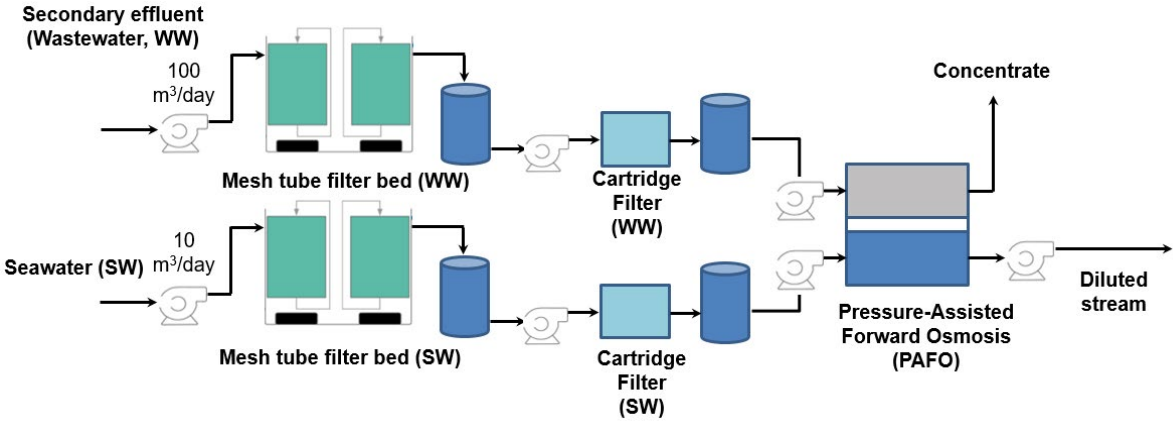

Fig. 1. Process flow chart of the FO pilot system with the location of equipped devices.

Table 1
Characteristic of seawater and secondary wastewater effluent

Water quality parameter	Secondary wastewater effluent		Seawater	
	Raw	Treated	Raw	Treated
Turbidity (NTU)	2.2 ± 5.7	0.6 ± 0.12	0.6 ± 0.32	0.2 ± 0.09
TOC (mg/L)	5.5 ± 0.09	5.2 ± 0.2	1.7 ± 0.01	1.6 ± 0.03
SS (mg/L)	5 ± 1.09	3 ± 1.4	2.4 ± 0.6	0.8 ± 0.7
TDS (mg/L)	3,319 ± 161		32,258 ± 242	
SDI	N/A	N/A	3.7 ± 0.2	2.4 ± 0.2

(Grundfos, Product: CRN10–14 A-FGJ-G-E-HQQE and CRN3–5 A-FGJ-G-E-HQQE, Denmark) equipped in the system for feed and draw streams. The automated pressure valve (FCI DeltaPValve, G-TECH. ENG, Korea) was installed at the outlet of the feed side. The pilot system is fully controlled by the supervisory control and data acquisition (SCADA) system. In connection with the SCADA system, automated pressure valve, feed and draw pumps enable automatic operation, maintaining constant feed outlet pressure, feed flow rate and draw flowrate regardless of any hydrodynamic changes that occurred during long-term operation. Pressure gauges (Endress+Hauser, Cerabar S, Switzerland), flowmeters (Endress+Hauser, PROMAG 10, Switzerland), and total dissolved solids (TDS) meters (Georg Fischer, Signet 9900 Transmitter, Switzerland) were installed to monitor the variation of pressure, flow rate and concentration. According to our previous works [9,13], more than 3 of FO membrane elements in serial connection can be inefficient in terms of draw stream dilution and subsequent RO energy cost reduction. Accordingly, 3 elements, stored in a separate pressure vessel (ROPV, R8040B300S-1W 1D5D, maximum pressure = 21 bar, China), were serially connected to analyze the performance of PAFO operation. Feed and draw streams were not recirculated but operated in a one-way direction.

2.4. Operating conditions

For an extensive evaluation of the effect of feed, draw flowrates and hydraulic pressure on behaviors of water flux and diluted concentrations, a wide range of flowrate and hydraulic conditions were utilized for performance analysis. Feed flowrates and draw flowrates varies from 10 to 70 LPM, and 2.5 to 7.5 LPM respectively for all serial configurations and hydraulic pressures varies 0–4 bar, 0–2 bar and 0–1 bar for single element (SE1), two elements (SE2) and three elements (SE3) in serial connection respectively. Throughout operation temperature of water varied as 22 ± 0.7 and 18.5 ± 0.6 for feed and draw solutions respectively. The duration of each operation for designated operating conditions was set to be 30 min. Hydraulic pressure is defined as the pressure difference between outlet feed pressure and inlet draw pressure of the last element.

Averaged water flux in each membrane element was computed based on the following equation:

$$J_w = \frac{Q_{D,\text{out}} - Q_{D,\text{in}}}{A_m} \quad (1)$$

where J_w is averaged water flux (L/m^2/h), A_m is total membrane area in a single element (m^2), $Q_{d,\text{out}}$ and $Q_{d,\text{in}}$ (LPM) are draw flowrate measured at inlet and outlet respectively.

3. Results and discussion

3.1. Variation of water flux under varying operating conditions

Fig. 2 illustrates water flux variations under varying feed flowrates (10–70 LPM), draw flowrates (2.5–7.5 LPM) and hydraulic pressures (0–4 bar) in a single element operation. Under each pressure condition, cumulative average water flux varied 9.89–15.21, 11.78–16.96, 13.89–18.83, 14.96–21.17 and 16.61–21.13 LMH for 0–4 bar of applied hydraulic pressure. Generally, water flux increases with increasing both feed and draw flowrates, but they are different in the extent of contribution to water flux increase. In spite of the narrow range of varied flowrate, draw flowrate showed a more significant influence on water flux variation than that of varied feed flowrate. According to previous studies based on pilot-scale FO operation [9,15], feed flowrate has a negligible effect on water flux improvement. Although the effect of feed flow rate was relatively insignificant compared to the effect of draw flowrate in the current results, feed flowrate showed a noticeable effect on water flux variation as shown in Fig. 2. This may be attributed to different feed concentration and ion compositions between artificial and real wastewater. As shown in Table 1, the TDS concentration of secondary waste effluent used in the current study is 3,319 ± 161 mg/L, which is significantly higher than the concentration of tap water (200 mg/L) used in other pilot studies. Higher feed concentration induces a higher degree of concentrative external concentration polarization (CECP) that reduce resulting water flux [16]. According to [17], the degree of external concentration polarization can be controlled under varying cross-flow velocities. This high concentration on the membrane surface on the feed side can explain the different extent of dependency of feed flowrate on resulting water flux. Particularly, water flux was notably low under 20 LPM of feed flow rate in all the pressure conditions in a single element and such trend become more pronounced as increasing hydraulic pressure. This means 20 LPM is the minimum feed flowrate to provide sufficient water volume to permeate through membrane that induces water flux. The higher dependency of draw flowrate on water flux implies that dilutive external concentration polarization (DECP) on the draw side is much more sensitive than CECP in the feed side due to significant difference in bulk concentrations between feed and draw streams.

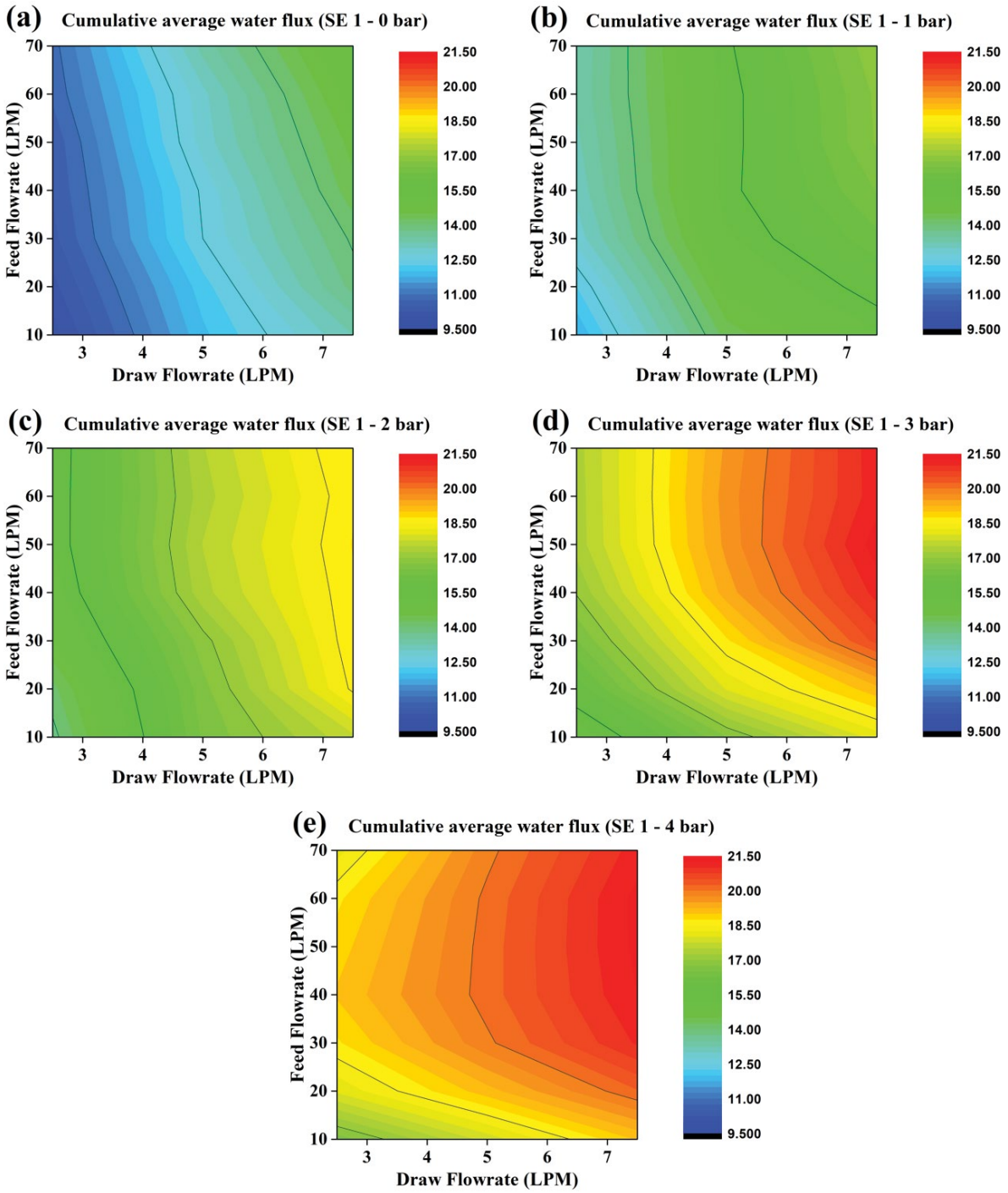

Fig. 2. Variation of cumulative average water flux in a single element (SE1) under varying feed, draw flowrates under 0 bar (a), 1 bar (b), 2 bar (c), 3 bar (d) and 4 bar (e) of hydraulic pressure.

Fig. 3 depicts water flux variation under varying operating conditions in serially-connected multiple elements. Under each pressure conditions, cumulative average water flux varies 20.4–28.48, 21.83–32.19 and 24.54–37.12 LMH for 0–2 bar of hydraulic pressure in SE2 and 14.32–41.56 and 24.07–49.85 LMH for 0–1 bar of hydraulic pressure in SE3. Similarly, 20 LPM seems to be a minimum feed flowrate to produce water flux effectively. As feed flowrate showed a certain boundary that determines efficiency in creating water flux, draw flowrates also seem to have such boundary at around 5 LPM in a serial configuration. As shown in Fig. 3, water flux notably increases above 5 LPM of draw flowrate. This means 5 LPM is the minimum draw flowrate to efficiently produce water flux by reducing the extent of DECP. Although this flowrate boundary (i.e. 20 LPM of feed flowrate and 5 LPM of draw

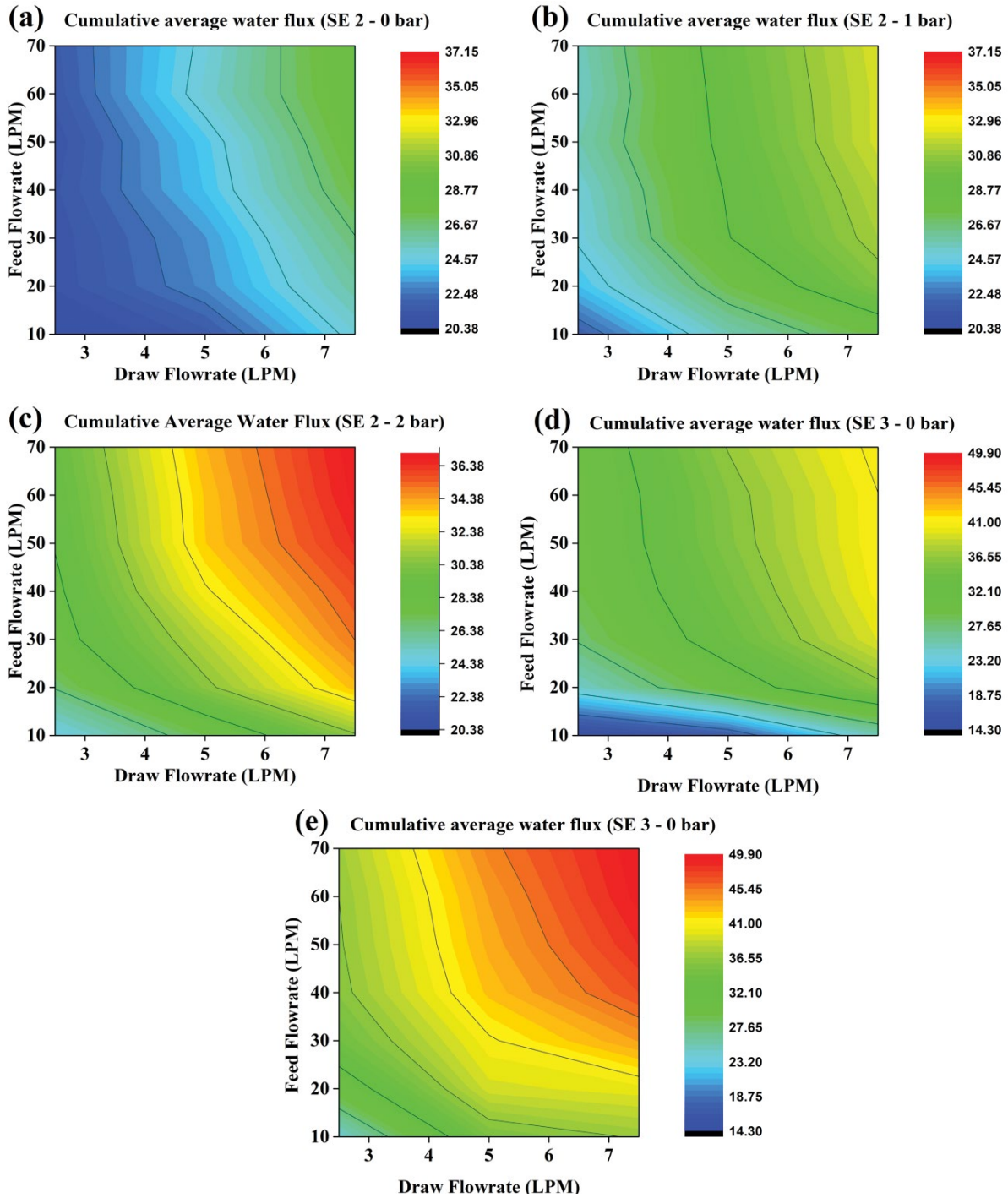

Fig. 3. Variation of cumulative average water flux in a serial configuration under varying feed, draw flowrates under 0 bar (a), 1 bar (b), 2 bar (c) in SE2 and 0 bar (d), 1 bar (e) in SE3.

flowrate) can change depending on the extent of CECP and DECP respectively, these boundaries maintained constantly throughout given operating conditions in the results.

For a clear illustration of pressure dependency on water flux, the average value of water fluxes measured in each different feed and draw flowrates was computed and plotted for each pressure condition and number of elements in Fig. 4. Variation of water flux by flowrates was expressed as error bars in graphs. Compared to SE2 and SE3, SE1 shows a relatively gradual slope and especially after 3 bar water flux improvement by hydraulic pressure becomes negligible. On the other hand, with an increasing number of elements, the effect of pressure on water flux improvement increased. This is probably because a larger membrane area is more advantageous to receive pressure benefit that induces effective hydraulic pressure to increase water flux regardless of

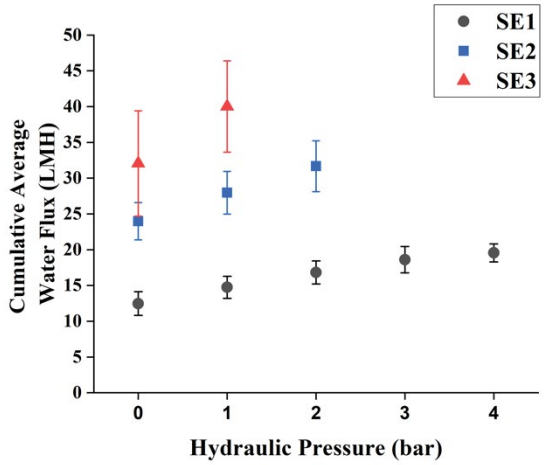

Fig. 4. Cumulative average water flux depending on hydraulic pressure and a different number of elements in a serial configuration. Error bars were drawn to show flux variation by feed and draw flowrates.

diminishing effective osmotic pressure as a number of elements increase. Furthermore, wider water flux variation by flowrates was observed with an increasing number of elements in serial. This is because water volume inside the feed channel gradually decreases due to water permeation to draw side as passing through serially-connected elements and becomes insufficient to efficiently produce water flux. Similarly, draw stream gradually become diluted as passing through elements and effective osmotic pressure decrease. For this reason, higher flowrates (either feed or draw) are required to fully derive water flux in a serial configuration, utilizing a higher membrane area. In other words, high feed and draw flowrates are desirable to fully exploit advantages of higher membrane area in serial configurations.

3.2. Variation of diluted draw concentration under varying operating conditions

Diluted draw concentration can be determined by mainly two factors, amount of water permeate (water flux) and retention time of draw stream (draw flowrate). Especially, several FO pilot studies [9,18] reported that draw flowrate has a significant effect on diluted draw concentration. Fig. 5 shows how diluted draw concentration varies depending on operating conditions in a single element. Each concentration was varied 16,000–23,111, 15,554–22,893, 15,412–22,437, 15,324–21,956 and 14,774–21,593 mg/L for 0–4 bar of applied hydraulic pressure. As discussed earlier, diluted concentration was dominated by draw flowrate and feed flowrate show minimal effect on concentration variation. Yet, higher diluted concentration was observed at low range of feed flowrate (10–20 LPM), which is attributed to low water flux behavior below 20 LPM of feed flowrate as discussed in the previous section.

Variation of diluted concentration in the serial configuration is depicted in Fig. 6. The concentration was varied 12,943–18,099, 11,868–18,118 and 10,362–16,487 mg/L for 0–2 bar of hydraulic pressure respectively in SE2 and 8,074–15,193 and 7,500–14,162 mg/L for 0–1 bar of hydraulic pressure in SE3. Compared to a single element, serial configurations show a similar pattern of concentration variation with similar standard deviation values (approx. 2,800 mg/L). This similar deviation value can be questionable when considering higher water flux induced from serial configuration compared to that from a single element. However, this can be explained by the difference in dilution efficiency at different draw concentration. To be clear, concentration that can be reduced at low concentration and high concentration of draw stream can differ when using the same amount of water permeate (water flux). In other words, as draw concentration gets lower higher water permeate is required to reduce the same extent of concentration. In this regard, Fig. 7 shows the pressure dependence of diluted draw concentration with different numbers of elements in serial. Each plotted value was computed as the average of concentration variation by feed and draw flowrates at designated pressure point. In SE1, the reduction of diluted concentration seems insignificant compared to SE2 and SE3, which can be attributed to minimal water flux improvement mentioned in the previous section. SE2 shows a relatively steep decrease compared to SE1 but slope in SE3 is relatively insignificant again, which is also attributed to the aforementioned dilution inefficiency at low draw concentration.

3.3. Performance discrepancy between artificial and field water condition

To compare performance of PAFO under artificial and field conditions (i.e. characteristics of feed and draw solution), Fig. 8 depicts by plotting water flux and diluted draw concentration values from [13], which was measured using artificial seawater (made of pure NaCl) as draw solution and tap water (200 mg/L) as feed solution and those measured under identical operating condition and using identical FO spiral-wound module (Toray FO 8040) but different water condition as given in Table 1. As clearly shown in Fig. 8a, overall water flux in field condition was almost half of that in artificial condition. Especially, in terms of pressure dependence on water flux, field conditions revealed a relatively weak correlation compared to artificial conditions. This significant difference in water flux pattern is mostly attributed to less bulk concentration difference between field and artificial conditions. Real seawater and wastewater used in the current study were approximately 3,000 mg/L lower and higher than artificial seawater and tap water respectively. In addition, the complex ion composition of real seawater can result in further deviation of effective osmotic pressure, creating an additional reduction of resulting water flux [19].

Fig. 8b shows a comparison of diluted draw concentration under the aforementioned artificial and field water condition. Compared to the significant difference in water flux in Fig. 8a, diluted concentration showed relatively less difference between the two conditions. Especially, in multiple element configurations (SE2, SE3), the discrepancy was even smaller than that in a single element and field condition showed even less diluted concentration in SE3 and 0 bar of hydraulic pressure. On the other hand, SE1 showed a significant difference, especially, concentration difference become severer with increasing hydraulic pressure. The reason for less difference in diluted concentration than water

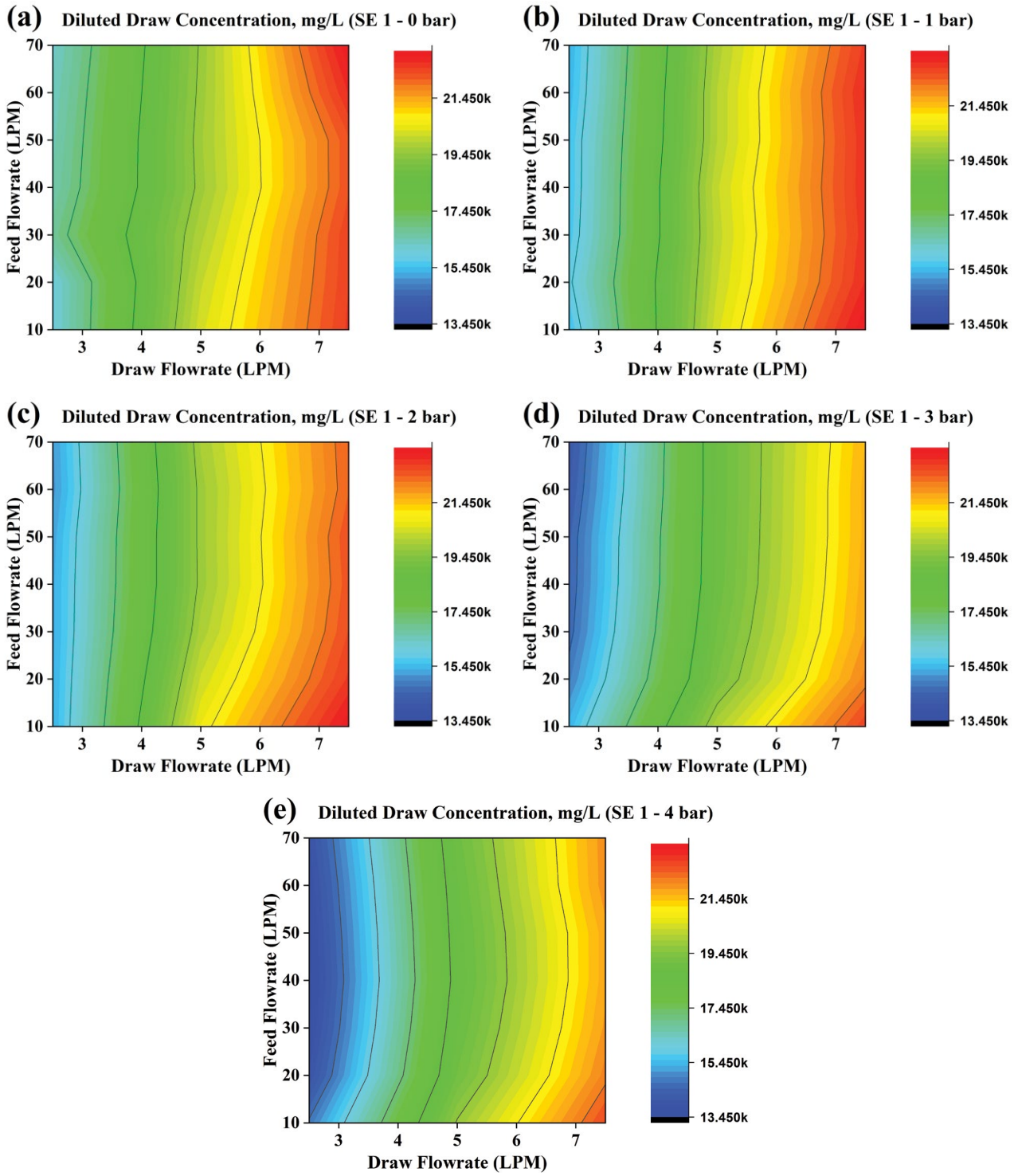

Fig. 5. Variation of diluted draw concentration in a single element (SE1) under varying feed, draw flowrates under 0 bar (a), 1 bar (b), 2 bar (c), 3 bar (d) and 4 bar (e) of hydraulic pressure.

flux between the two conditions can be explained originally low concentration of real seawater. As discussed earlier, the real seawater concentration used in the current study was approximately 32,000 mg/L, which allowing lower diluted concentration with approximately half of the water flux.

Since the majority of seawater has a concentration varying from 31,000 to 38,000 mg/L [20] and wastewater concentration varies from 1,000 to 10,000 mg/L [21] over the globe, this discrepancy in TDS concentration has to be considered to more precisely project performance of PAFO onto its

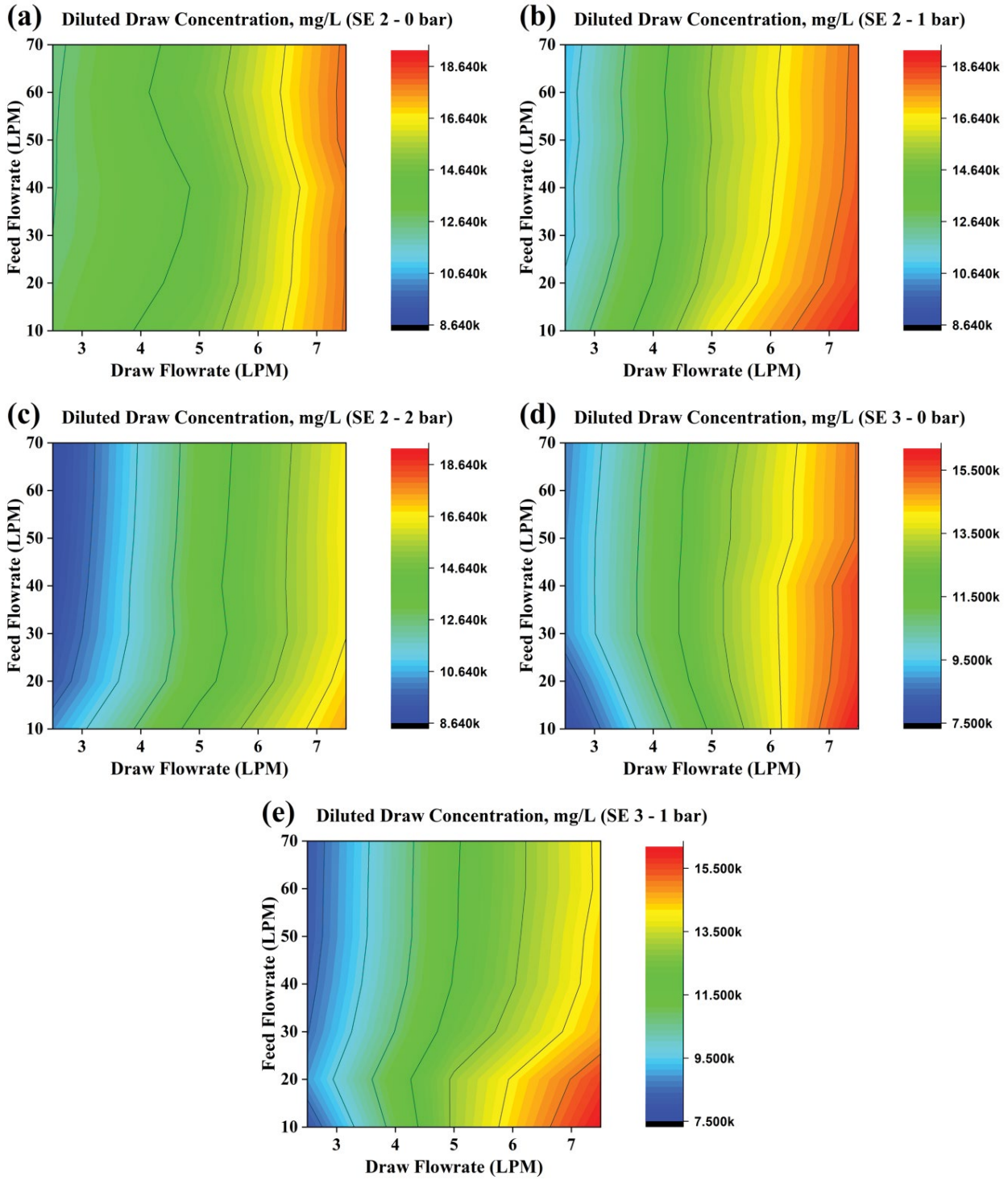

Fig. 6. Variation of diluted draw concentration in a serial configuration under varying feed, draw flowrates under 0 bar (a), 1 bar (b), 2 bar (c) in SE2 and 0 bar (d), 1 bar (e) in SE3.

economic feasibility. Especially, due to the nature of the osmotically-driven process, which is that resulting water flux is way more sensitive to concentration condition than RO [1], this point cannot be neglected for practical and reliable performance evaluation.

4. Conclusion

In the current study, the performance of serially-connected FO spiral-wound elements using real seawater and wastewater under an extensive range of operating conditions (feed, draw flowrates and hydraulic pressure) were analyzed

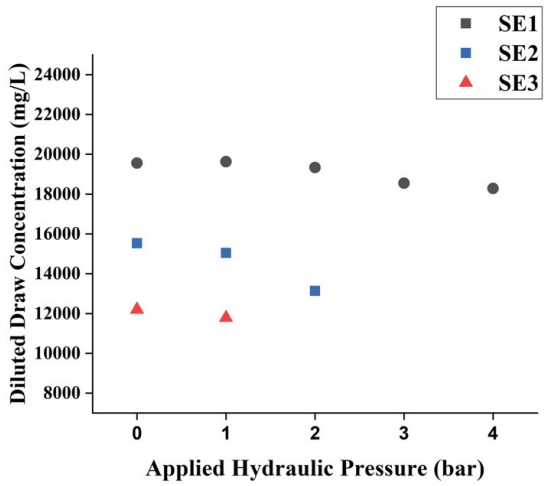

Fig. 7. Diluted draw concentration depending on hydraulic pressure and a different number of elements in serial connections.

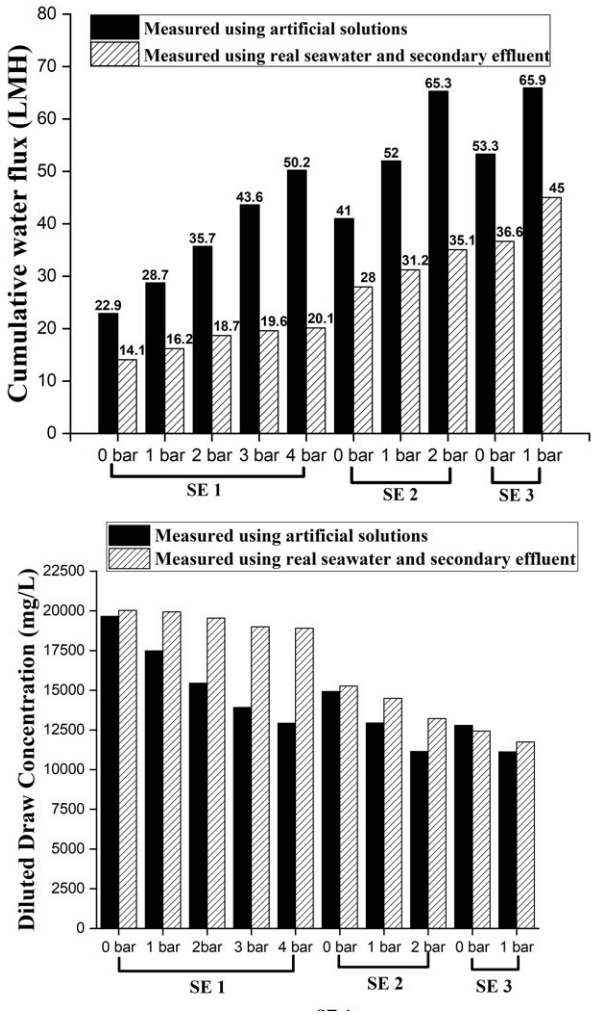

Fig. 8. Comparison of performance of serially-connected FO 8040 spiral-wound elements between when artificial solutions and real seawater and wastewater used (a) cumulative water flux and (b) diluted draw concentration, respectively.

and discussed. Behaviors of water flux and diluted concentration were analyzed in relation to each operating and water conditions. In all given operating conditions, 20 LPM of feed flowrate and 5 LPM of draw flowrate seem to be maximum flowrate for efficient production of water flux regardless of hydraulic pressure and number of elements in serial as there is no further significant improvement above those flowrate conditions. Given results also revealed a substantial difference between performance in artificial and field water conditions. Overall, water flux values in field conditions were approximately half of those in artificial water conditions due to the difference in feed and draw concentrations and complex water chemistry. Nonetheless, diluted concentration showed a relatively small discrepancy between the water conditions due to the low initial concentration of real seawater. Such deviation of pilot-scale PAFO performance between artificial and field water conditions cannot be discounted as it can derive meaningful disparity with an existing economic assessment of FO-RO or PAFO-RO hybrid based on artificial water conditions. Further investigation on economic assessment based on the performance under field water condition is therefore recommended for more practical insight on economic feasibility.

Acknowledgment

This work was supported by the Korea Environment Industry & Technology Institute (KEITI) through the Industrial Facilities & Infrastructure Research Program, funded by the Korea Ministry of Environment (MOE) (1485016165).

References

[1] H.K. Shon, S. Phuntsho, T.C. Zhang, R.Y. Surampalli, Forward Osmosis – Fundamentals and Applications, ASCE (American Society of Civil Engineers), Reston, Virginia, U.S., 2015.
[2] D.L. Shaffer, J.R. Werber, H. Jaramillo, S. Lin, M. Elimelech, Forward osmosis: where are we now?, Desalination, 356 (2015) 271–284.
[3] D.L. Shaffer, N.Y. Yip, J. Gilron, M. Elimelech, Seawater desalination for agriculture by integrated forward and reverse osmosis: improved product water quality for potentially less energy, J. Membr. Sci., 415–416 (2012) 1–8.
[4] G. Blandin, A.R.D. Verliefde, C.Y. Tang, A.E. Childress, P. Le-Clech, Validation of assisted forward osmosis (AFO) process: impact of hydraulic pressure, J. Membr. Sci., 447 (2013) 1–11.
[5] Y. Oh, S. Lee, M. Elimelech, S. Lee, S. Hong, Effect of hydraulic pressure and membrane orientation on water flux and reverse solute flux in pressure assisted osmosis, J. Membr. Sci., 465 (2014) 159–166.
[6] G. Blandin, A.R.D. Verliefde, P. Le-Clech, Pressure enhanced fouling and adapted anti-fouling strategy in pressure assisted osmosis (PAO), J. Membr. Sci., 493 (2015) 557–567.
[7] S.J. Im, S. Jeong, A. Jang, Feasibility evaluation of element scale forward osmosis for direct connection with reverse osmosis, J. Membr. Sci., 549 (2018) 366–376.
[8] J.E. Kim, S. Phuntsho, S.M. Ali, J.Y. Choi, H.K. Shon, Forward osmosis membrane modular configurations for osmotic dilution of seawater by forward osmosis and reverse osmosis hybrid system, Water Res., 128 (2018) 183–192.
[9] S. Kook, J. Kim, S.-J. Kim, J. Lee, D. Han, S. Phuntsho, W.-G. Shim, M. Hwang, H.K. Shon, I.S. Kim, Effect of initial feed and draw flowrates on performance of an 8040 spiral-wound forward osmosis membrane element, Desal. Wat. Treat., 72 (2017) 1–12.

[10] J. Kim, G. Blandin, S. Phuntsho, A. Verliefde, P. Le-Clech, H. Shon, Practical considerations for operability of an 8″ spiral wound forward osmosis module: hydrodynamics, fouling behaviour and cleaning strategy, Desalination, 404 (2017) 249–258.
[11] G. Blandin, A. Verliefde, P. Le-Clech, Pressure-assisted osmosis (PAO)–RO hybrid: impact of hydraulic pressure on fouling and economics, Desal. Wat. Treat., 55 (2015) 3160–3161.
[12] R. Valladares Linares, Z. Li, V. Yangali-Quintanilla, N. Ghaffour, G. Amy, T. Leiknes, J.S. Vrouwenvelder, Life cycle cost of a hybrid forward osmosis - low pressure reverse osmosis system for seawater desalination and wastewater recovery, Water Res., 88 (2016) 225–234.
[13] S. Kook, C. Lee, T.T. Nguyen, J. Lee, H.K. Shon, I.S. Kim, Serially connected forward osmosis membrane elements of pressure-assisted forward osmosis-reverse osmosis hybrid system: process performance and economic analysis, Desalination, 448 (2018) 1–12.
[14] B.G. Choi, M. Zhan, K. Shin, S. Lee, S. Hong, Pilot-scale evaluation of FO-RO osmotic dilution process for treating wastewater from coal-fired power plant integrated with seawater desalination, J. Membr. Sci., 540 (2017) 78–87.
[15] Y.C. Kim, S.J. Park, Experimental study of a 4040 spiral-wound forward-osmosis membrane module, Environ. Sci. Technol., 45 (2011) 7737–7745.
[16] J.R. McCutcheon, R.L. McGinnis, M. Elimelech, Desalination by ammonia-carbon dioxide forward osmosis: influence of draw and feed solution concentrations on process performance, J. Membr. Sci., 278 (2006) 114–123.
[17] M.F. Gruber, C.J. Johnson, C.Y. Tang, M.H. Jensen, L. Yde, C. Hélix-Nielsen, Computational fluid dynamics simulations of flow and concentration polarization in forward osmosis membrane systems, J. Membr. Sci., 379 (2011) 488–495.
[18] S.J. Im, G.W. Go, S.H. Lee, G.H. Park, A. Jang, Performance evaluation of two-stage spiral wound forward osmosis elements at various operation conditions, Desal. Wat. Treat., 57 (2016) 24583–24594.
[19] D. Stigter, T.L. Hill, Theory of the Donnan membrane equilibrium. II. Calculation of the osmotic pressure and of the salt distribution in a Donnan system with highly charged colloid particles, J. Phys. Chem., 63 (1959) 551–555.
[20] F.J. Millero, R. Feistel, D.G. Wright, T.J. McDougall, The composition of standard seawater and the definition of the reference-composition salinity scale, Deep Sea Res. Part I, 55 (2008) 50–72.
[21] H. Mirbolooki, R. Amirnezhad, A.R. Pendashteh, Treatment of high saline textile wastewater by activated sludge micro-organisms, J. Appl. Res. Technol., 15 (2017) 167–172.